Chemistry Africa (2020) 3:127–134
https://doi.org/10.1007/s42250-019-00097-4

ORIGINAL ARTICLE

Structured Magnetic Core/Silica Internal Shell Layer and Protein Out Layer Shell (BSA@SiO_2@SME): Preparation and Characterization

Mohamad Tarhini[1] · Jaime Vega-Chacón[1,2] · Miguel Jafelicci Jr.[2] · Nadia Zine[3] · Abdelhamid Errachid[3] · Hatem Fessi[1] · Abdelhamid Elaissari[1]

Received: 11 July 2019 / Accepted: 1 October 2019 / Published online: 10 October 2019

Abstract

Purpose Magnetic nanoparticles are an interesting approach in the biomedical and biotechnological field. They can be used as a drug delivery system or in magnetic resonance imaging. However, these particles have the disadvantage of being colloidally instable, easily oxidized, and suffer from partial toxicity. To overcome these problems, magnetic nanoparticles were coated by different types of coats such as silica, polymer, etc. the purpose of this study is to develop a coated iron oxide nanoparticle system.

Methods Seed magnetic emulsion particles (SME) were first prepared and characterized before inducing silica layer using sol–gel process. The obtained SiO_2@SME particles are then encapsulated using bovine serum albumin (BSA) layer. This proteins layer was performed via nanoprecipitation of BSA molecules on the SME. Particles were characterized by electron microscopy, FTIR, TGA, and zeta potential measurement.

Results Characterization studies confirm the successful coating of BSA on the surface of amino-functionalized silica shell and magnetic core.

Conclusion The used process leads to the preparation of highly magnetic particles encapsulated with silica layer ad then coated with proteins shell. The presence of silica shell will enhance the chemical stability of the magnetic core, whereas, the presence of proteins shell will improve low cytotoxicity and good biocompatibility in the contact with biological samples.

Keywords Bovine serum albumin · Nanoparticle · Iron-oxide · Core–shell · Coating · Encapsulation · Nanoprecipitation

1 Introduction

Magnetic nanoparticles have gained much attention in the biomedical field, targeted drug delivery, and bio-imaging due to their ability to respond to magnetic field [1]. Magnetic particles made from iron oxide are particularly important because of their availability and manufacturing simplicity. In addition, these particles feature a superparamagnetic behavior. Briefly, they are only magnetized in the presence of a magnetic field. While their magnetization is zero in the absence of the latter. This property gives the nanoparticles an extra stability when dispersed in solution [2].

Magnetic nanoparticles were prepared via various techniques such as co-precipitation, micelle synthesis, hydrothermal synthesis, thermal decomposition, etc. [3–7]. Nanoparticles were produced with a low size range (2–100 nm) allowing the easy penetrability through biological barriers [8, 9]. However, particles in this size range suffer from colloidal and chemical instability at a long term. These particles tend to form agglomerates to reduce the energy of the system caused by the high surface area/volume ratio. In addition, metallic nanoparticles in general are chemically highly active, and can be easily oxidized in air which may lead to the loss of magnetization and dispersibility [10]. Solutions were suggested to solve this problem, such as coating the particles with different materials, organic or inorganic, such as surfactants, polymer, or silica [10]. This coating step, can chemically stabilize magnetic particles against degradation as a function of time. In addition, coating can be used for

✉ Abdelhamid Elaissari
abdelhamid.elaissari@univ-lyon1.fr

[1] Univ Lyon, University Claude Bernard Lyon-1, CNRS, LAGEP-UMR 5007, 69622 Lyon, France

[2] Institute of Chemistry, São Paulo State University (UNESP), Araraquara, São Paulo, Brazil

[3] Institute of Analytical Sciences, UMR 5280, Claude Bernard Lyon 1 University, University of Lyon, Villeurbanne, France

the functionalization of the nanoparticles surface, where different substances and ligands can be added to enhance the colloidal stability and targeting specificity [11].

Protein based nanoparticles (PBN) have also gained some attention as drug carriers for several reasons. Proteins are natural biopolymers that are widely available in nature, they are completely non-toxic, biodegradable, and do not leave undesirable biodegradation products. Among protein, albumin has a paramount importance, since its natural role as a transporter protein gave it the ability to bind to a large spectrum of drugs and ligands for better specificity. Bovine serum albumin (BSA)-based particles were heavily studied and synthesized with different techniques such as nanoprecipitation, emulsification, self-assembly, etc. depending on the method and the experimental parameters, the size of BSA nanoparticles ranges between 50 and 250 nm. These types of protein-based particles are of good colloidal stability, easy to prepare and to control the colloidal properties [12].

For the above reasons, BSA-coated magnetic nanoparticles were previously studied by Li et al. by coating iron oxide nanoparticles (Fe_2O_4) by BSA shell. The shell is obtained via adsorption process. The produced nanoparticles have a diameter of 35 nm and a narrow size distribution. In addition, these nanoparticles have a spherical morphology and the BSA was proved to be present on the surface of the magnetic nanoparticles. These results showed the feasibility of the magnetic protein nanoparticle formulation [13]. In addition, it was proved that BSA coating leads to good toxicological profile and good biodistribution of the magnetic nanoparticles [14]. Moreover, this approach may give the particles the long-term stability and the ligand binding ability, all with preserving the magnetic properties of the iron oxide core. In another study, produced nanoparticles have a diameter of 25 nm and a zeta potential of − 26 mV. In addition, microscopy images suggest the presence of a monolayer coating the iron oxide core. Results show that coating with BSA decreases the degradation of the nanoparticles and reduces the toxicity in the animal model [14]. Another study showed that BSA coating of an iron oxide core can improve the in vivo and in vitro therapeutic outcome for efficient cancer treatment [15, 16].

Firstly, it's interesting to notice that, in this manuscript that we are not performing adsorption of proteins on magnetic nanoparticles (10 to 100 nm), but we are performing nanoprecipitation of proteins on the used magnetic seed emulsion (300 to 500 nm). In this study, magnetic seed emulsion was first coated with silica layer bearing amine groups and then encapsulated by BSA shell through a simple method based on protein precipitation where higher amount of BSA was used comparing to previous studies. By using FTIR, TGA, zeta potential measurement, transmission electron microscopy, and magnetization measurement, the physico-chemical properties and the surface modification in each step of preparation were evaluated and the precipitation of BSA on the magnetic core was investigated.

2 Experimental

2.1 Materials and Reagents

Iron (III) chloride hexahydrate ($FeCl_3{\cdot}6H_2O$), iron (II) chloride tetrahydrate ($FeCl_2{\cdot}4H_2O$), oleic acid, bovine serum albumin (BSA, 96%) and sodium dodecyl sulfate (SDS) were purchased from Sigma-Aldrich and used without purification. Ammonia solution (NH_4OH, 25%) and ethanol (96%) were purchased from VWR Prolabo and used as received. Polyvinylpyrrolidone (PVP) and tetraethyl orthosilicate (TEOS) were obtained from Fluka. Octane and (3-aminopropyl)triethoxysilane (APTS, 99%) were obtained from Acros Organics. Acetone was purchased from Laurylab. Deionized water was used over all the experiments. Polyoxyethylene (40) isooctylphenyl ether (Triton X-405), NaOH and HCl solution are products of Sigma-Aldrich and Sodium dodecyl sulphate (SDS) was from ProLabo.

2.2 Preparation of oil in water magnetic emulsion (SME)

The synthesis of organic ferrofluid was carried according to Montagne et al. [17]. In brief, nanoprecipitation process of ferric and ferrous salts and by transferring the obtained nanoparticles into organic phase using oleic acid was done. Then, the organic ferrofluid were emulsified using Triton X-405 and SDS in order to obtain stable, submicron, narrowly size distributed oil in water magnetic emulsion. The obtained oil in water magnetic emulsion was thermally treated in order to remove the organic solvent and to obtain thermodynamically stable magnetic dispersion. Then, the final magnetic particles (SME) are solvent free.

2.3 Preparation of Silica Coated Seed Magnetic Emulsion (SiO_2@SME)

Silica coated SME were prepared according to Bitar et al. [18]. Briefly, the above-mentioned oil in water magnetic emulsion particles were separated by magnet from 3 ml emulsion (9.6% w/v) after organic solvent evaporation. The particles were washed by deionized and redispersed in 0.9 ml PVP aqueous solution (10% w/v). The prepared dispersion (SME) was kept on rotation agitation for 3 h. Then, 1.5 ml NH_4OH (25%) were added to the emulsion and the agitation continued for 15 min. Next, 0.75 ml TEOS were dissolved in 0.3 ml ethanol, this solution was added to the SME and kept under stirrer for one night. The obtained SiO_2@SME particles were separated by magnet and washed by deionized water.

2.4 Preparation of Amino-Functionalized Silica Coated Seed Magnetic Emulsions (APTS@SiO_2@SME)

The surface modification of the nanoparticles was carried out through silanization process using APTS, in order to introduce amino groups at the nanoparticles surface. 0.25 g of SiO_2@SME nanoparticles were dispersed by sonication in 80 ml of water–ethanol solution (1:1 v/v). The pH of the suspension was adjusted to 9.0 with the addition of ammonia solution. Under magnetic stirring, 145 µl of APTS was added to the suspension and allowed to react for 1 h at 40 °C. The particles were magnetically collected from the dispersed suspension with an external magnetic field and washed with ethanol. The collected magnetic particles were dispersed by sonication in deionized water. Dried samples were obtained by lyophilization.

2.5 Preparation of BSA Coated SME Nanoparticles (BSA@SiO_2@SME)

Two BSA aqueous solutions at 6% and 4% (w/v) were prepared. These solutions were then added separately to an APTS@SME suspension (4%) with an equal volume. This leads to the formation of two mixtures of BSA and APTS@SME nanoparticles with 2% APTS@SME nanoparticles (w/v) for both, and 3% BSA and 2% BSA (w/v) respectively. Ethanol (non-solvent) was added in these two samples under stirring at room temperature with a solvent/non-solvent ratio of 1/2 to induce the precipitation of BSA. After that, ethanol was eliminated by rotary evaporation in both samples. The particles were magnetically separated from the supernatant and washed with water three times. Dried samples were obtained by lyophilization. The obtained nanoparticles were named as BSA2@SME and BSA3@SME, the number indicates the concentration of BSA in the preparation mixture.

2.6 Samples Characterization

FTIR analyses were performed by FTIR spectrophotometer Nicolet iS50 FTIR (Thermo Scientific) in the ATR mode. Nanoparticle suspension was dropped onto the ATR crystal and left to dry prior to analysis. The spectra were scanned over the range 4000–500 cm^{-1}.

The surface charge of the nanoparticles was determined by measurements of zeta potential using Zetasizer Nano ZS equipment. Zeta Potential was measured as a function of pH in a range 2.5–10.5 at room temperature. Particles were dispersed in 5 mmol l^{-1} NaCl aqueous solution. Zeta potential was measured taking an average of three measures. The zeta potential of BSA nanoparticles prepared according to Tarhini et al. [19] were analyzed too for comparing with the synthesized particles.

Thermogravimetric analysis (TGA) of dried samples was performed by TG 209 F1 ASC (Netzsch) equipment from 25 °C up to 800 °C at a heating rate of 10 °C min^{-1} under a nitrogen flow rate of 20 ml min^{-1}.

Transmission electron microscopy (TEM) images were obtained with a Phillips CM120 electron microscope (Claude Bernard University-Lyon1, CTµ, Lyon, France). One drop of highly diluted particles was placed onto a copper grid (mesh 200 and covered with formvar-carbon) and dried at room temperature before TEM analysis. The analyses were performed with a field emission gun operating at 100 kV.

Magnetization measurements were carried out using the Automatic Bench of Magnetic Measurements (ABMM) at CNRS-IRC Lyon laboratory, France. Samples were dried and magnetization was investigated at room temperature by varying the magnetic field (H) from − 20,000 to + 20,000 Oersted.

3 Results and Discussion

Silica coated seed magnetic emulsions functionalized with amino groups and coated with BSA were prepared (Fig. 1). These particles were characterized, and evidence on the structure complexity was identified through different techniques.

Figure 2 displays the FTIR spectra of BSA, SiO_2@SME, BSA2@SME and BSA3@SME. BSA presents two characteristic bands at 1640 and 1520 cm^{-1}, which are attributed to amide I and amide II vibration modes, respectively. Bands at 3280 and 3060 cm^{-1} are assigned to –OH and –NH stretching vibration. Bands at 2960, 2930 and 2870 cm^{-1} are related to –CH stretching [13, 20–22].

Sample SiO_2@SME exhibits intense bands at 1065 and 560 cm^{-1} that are assigned to the Si–O–Si and the Fe–O stretching vibration due to the presence of silica and iron oxide. The bands at 3320 and 1630 cm^{-1} correspond to stretching and bending vibrations of hydroxyl on the nanoparticles surface [18, 23]. Sample SiO_2@SME and APTS@SME (not shown in the figure) present a similar spectrum, which indicates the deposition of a thin layer of SiO_2 in SiO_2@SME to form APTS@SME. Also, the characteristics bands of amino group are overlapped by the bands related to hydroxyl group, so the presence of amino group is confirmed by other method. Samples BSA2@SME and BSA3@SME present a similar spectrum and exhibit the characteristic bands of BSA, iron oxide and silica, which confirms the presence of these materials on the samples.

Thermogravimetric analysis was performed to determine the amount of BSA in samples BSA2@SME and BSA3@SME. TGA curves of SiO_2@SME, APTS@SME,

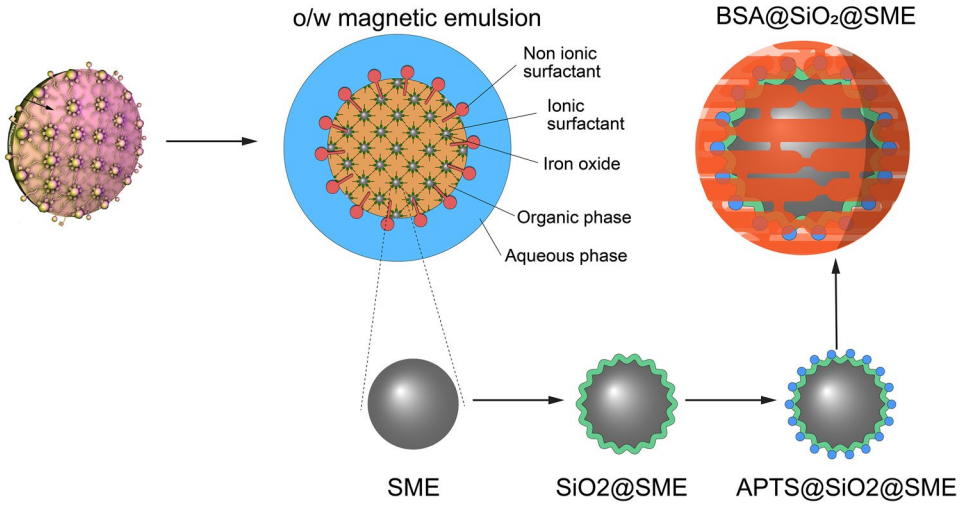

Fig. 1 The different steps for the preparation of BSA coated-amino functionalized-silica coated-SME nanoparticles

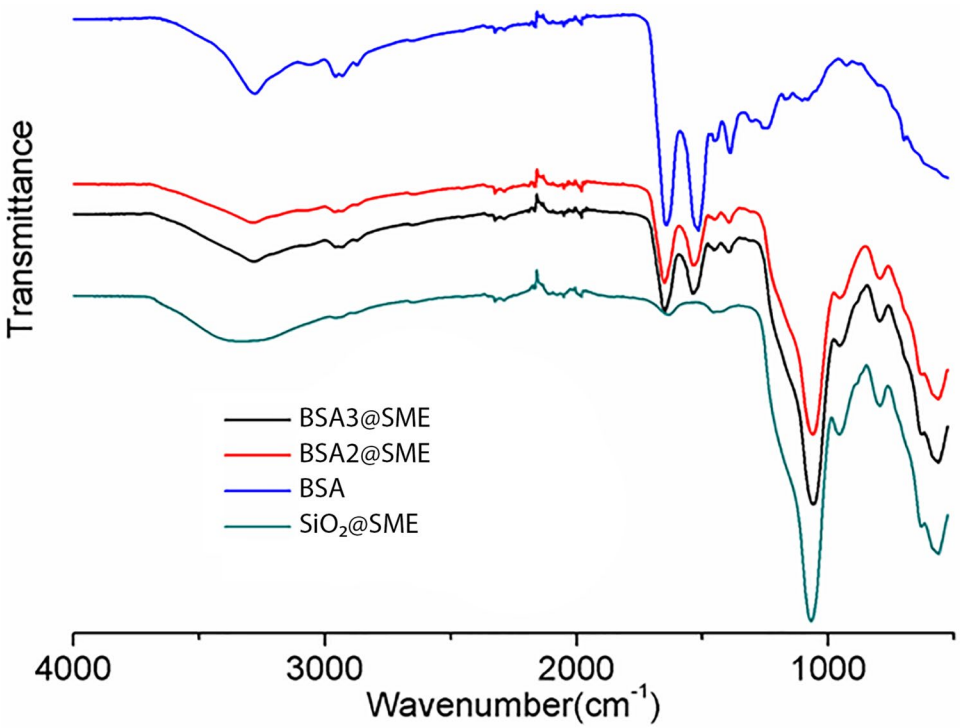

Fig. 2 FTIR spectra of bovine serum albumin (BSA), BSA@SME core–shell (BSA2@SME and BSA3@SME) and silica coated iron oxide nanoparticles (SiO2@SME)

BSA, BSA2@SME and BSA3@SME are shown in Fig. 3. The weight losses between 25 and 200 °C are attributed to the loss of water absorbed on the particles [21]. The water content in SiO_2@SME, APTS@SME, BSA, BSA2@SME and BSA3@SME is 3.6, 3.7, 6.0, 4.0 and 5.0%, respectively. The additional weight losses between 200 and 800 °C are related to the decomposition of organic material in each sample. The 7% of weight loss in SiO_2@SME corresponds to oleic acid molecules bonded on the surface of the iron oxide nanoparticles entrapped on the silica matrix [18].

The surface modification of SiO_2@SME with APTS introduced organic moieties with the amino group on the particles surface; this additional organic material was evidenced in the 11% of weight loss in sample APTS@SME [24, 25].

The decomposition of BSA starts at 200 °C, then the major weight loss of BSA occurs at about 300 °C and decompose completely at higher temperatures [26, 27].

Thermogravimetric analysis curve of BSA2@SME and BSA3@SME present a decomposition profile between 200 and 400 °C similar to BSA curve, which indicates the decomposition of the BSA attached on the nanoparticles surface. The weight loss that corresponds to organic material in

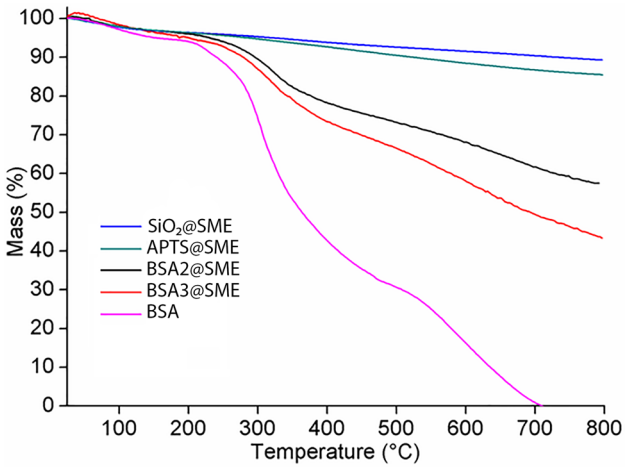

Fig. 3 TGA curves of SiO_2@SME, APTS@SME, BSA, BSA2@SME and BSA3@SME

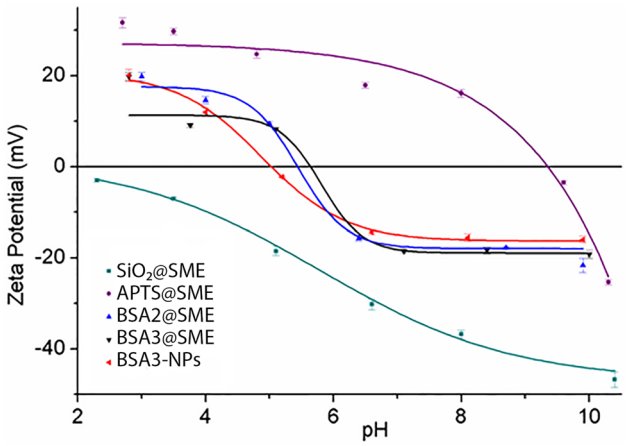

Fig. 4 Zeta potential as a function of pH of SiO_2@SME, APTS@SME, BSA2@SME, BSA3@SME and BSA-NP

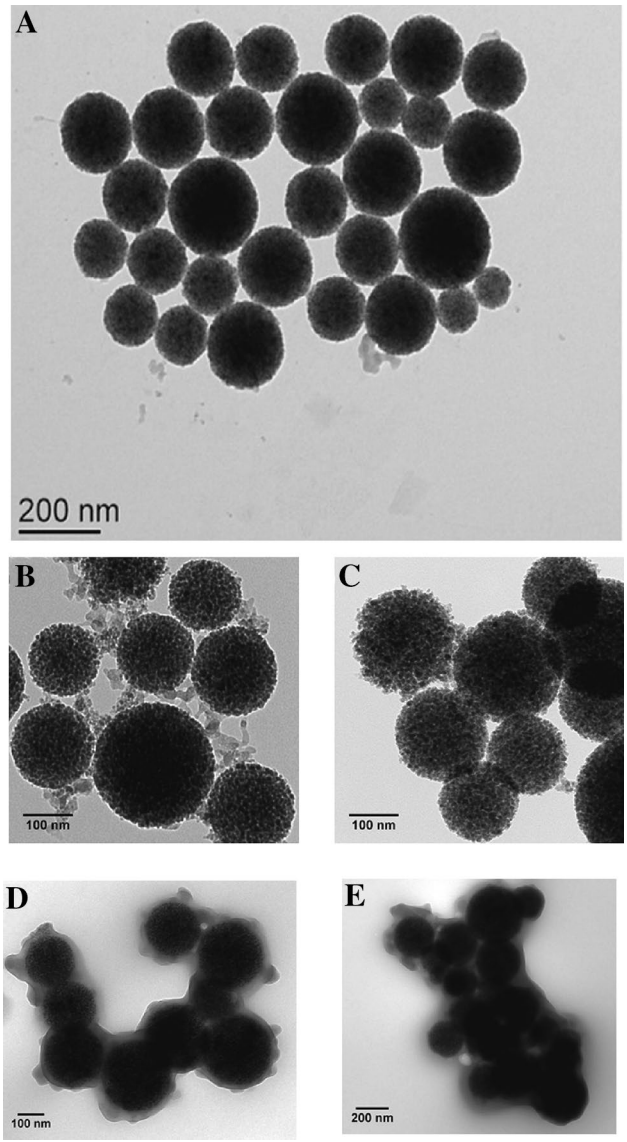

Fig. 5 TEM images: **a** SME, **b** SiO_2@SME, **c** APTS@SME, **d** BSA2@SME and **e** BSA3@SME

samples BSA2@SME and BSA3@SME is 38.3 and 51.8%, respectively. Then, considering the organic material that is presented in the APTS@SME nanoparticles, the estimated content of BSA in samples BSA2@SME and BSA3@SME is 30.7 and 45.8%, respectively. Previous works reported lower incorporations of BSA even when glutaraldehyde was used to chemically bond the BSA [13, 26, 28, 29].

Figure 4 represents the zeta potential curve of SiO_2@SME, APTS@SME, BSA2@SME, BSA3@SME and BSA-NP as a function of pH. The zeta potential is strongly influenced by the physico-chemical properties of the particles surface. The zeta potential curve of SiO_2@SME is similar to the zeta potential curve of silica particles, the isoelectric point (IEP, pH at which zeta potential is zero) seems to be close to 2, which is IEP of silica particles reported in previous works [18, 30]. This confirms the presence of silica on the surface of SiO_2@SME particles. The IEP of APTS@SME is 9.3, the increase in the IEP after the surface modification by APTS is produced by the presence of amino groups on the surface of APTS@SME particles [24, 25, 31]. The zeta potential curves of BSA2@SME and BSA3@SME are similar to the zeta potential curve of BSA particles (BSA-NP), these results verify the successful cover of magnetic particles by BSA. The IEP of BSA2@SME and BSA3@SME is 5.4 and 5.2, respectively, which are slightly higher than the IEP of BSA-NP (5.0). These differences in IEP probably are produced by the influence of amino groups presented on the magnetic particles. As the amount of BSA is higher in BSA3@SME than BSA2@SME, the influence

of amino groups related to the magnetic particles in the IEP is lower in BSA3@SME than in BSA2@SME.

Transmission electron microscopy images of samples SME, SiO_2@SME, APTS@SME, BSA2@SME and BSA3@SME can be observed in Fig. 5. SME particles were found to spherical in shape with wide size distribution (Fig. 5a). This observation is in accordance with the DLS measurement where a high polydispersity index was shown (about 0.8). SiO_2@SME exhibits spherical particles formed by aggregated iron oxide particles 9 nm, the average size of particles is 174 ± 20 nm. Although, zeta potential and FTIR analysis demonstrated the presence of silica on the surface, it cannot be observed a silica shell around the particles, this could indicate the formation of a thin silica layer on the surface. The introduction of amino groups on the particles surface did not produce appreciable changes on the size and shape of the particles. Samples BSA2@SME and BSA3@SME present structures formed by APTS@SME particles covered by an irregular material. As this material is brighter that the APTS@SME particles, it corresponds to a softer material which it was identified as BSA.

The magnetic behavior of the particles was evaluated by magnetization measurements. Figure 6 exhibit the magnetization curves of samples SiO_2@SME, APTS@SME, BSA2@SME and BSA3@SME. The samples exhibit the typical profile of superparamagnetic materials, since no hysteresis loops and no coercivity were observed in the curves. The saturation magnetization (the maximum of the magnetization value, Ms) of sample SiO_2@SME is 31.5 emu g^{-1} which is smaller than the corresponding to bulk phase (92 emu g^{-1}). Usually magnetic nanoparticles present lower value of Ms in comparison to the bulk phase [32, 33]. Ms is correlated to the proportion of magnetic material on the samples, when the surface modification of nanoparticles introduce non-magnetic material, the Ms of sample decreases [18, 34]. APTS@SME presents a Ms of 30.2 emu g^{-1}, which is just slightly lower than the Ms of SiO_2@SME, this result agrees with the previous thermogravimetric analysis that showed a low incorporation of non-magnetic material after the surface modification by APTS. The Ms of BSA2@SME and BSA3@SME is 24.0 and 21.7 emu g^{-1}, respectively. These results also agree with the large incorporation of organic material confirmed by thermogravimetric analysis. Although BSA2@SME and BSA3@SME present a lower value of Ms that bulk magnetite, it is enough for its applications in biomedical field.

4 Conclusion

Bovine serum albumin coated seed magnetic emulsion particles were prepared and the coating of the particles with BSA was investigated. The results of FTIR, thermogravimetric analysis, and zeta potential measurement, confirm the successful coating of BSA on the surface of amino-functionalized iron oxide particles. In addition, this can be observed by the transmission electron microscopy images. This study reports a successful coating of magnetic particles with a BSA shell using higher amounts than what can be found in literature. Using this process based on the preparation of well characterized oil in water magnetic emulsion, solvent evaporation, first encapsulation by silica layer and second

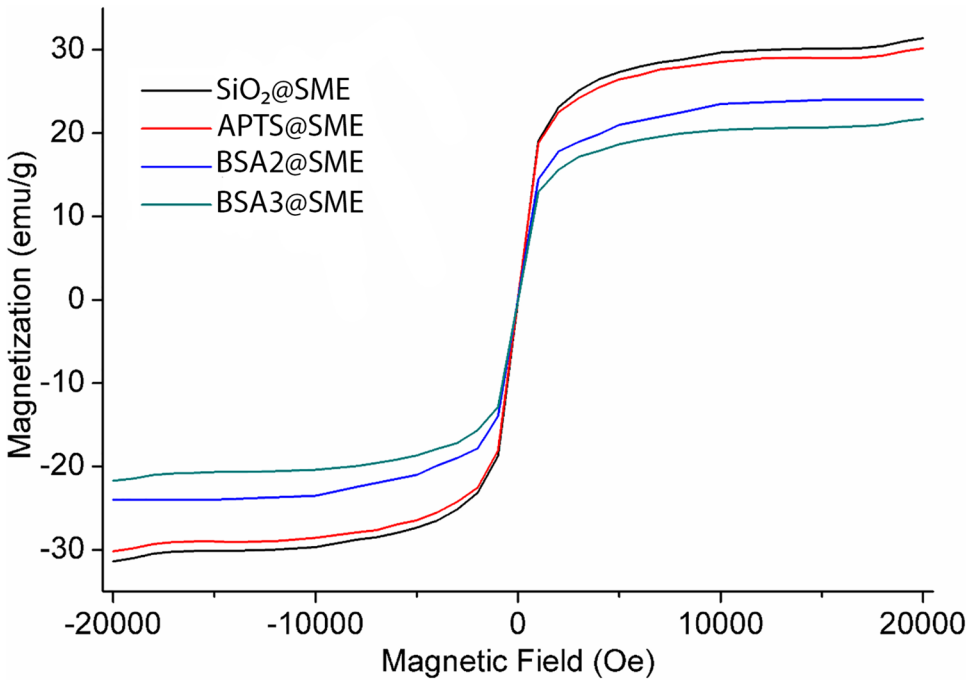

Fig. 6 Magnetization curve of SiO_2@SME, APTS@SME, BSA2@SME and BSA3@SME at 25 °C

encapsulation using BSA precipitation process leads to the preparation of well structured particles, submicron in size, highly magnetic and good colloidal stability for both in vitro and in vivo use. It's interesting to notice, that the particles size distribution is totally related to size distribution of the used seed magnetic emulsion.

Acknowledgements Jaime Vega-Chacón would like to thank Coordenação de aperfeiçoamento de pessoal de nivel superior (CAPES) for the Grant funded Bolsista capes/Programa Doutorado Sanduíche no Exterior/Processo n° {88881.132878/2016-01}. Funding was provided by Campus France (Grant No. PHC PROCOPE 40544QH), Horizon 2020 research and innovation programme entitled (An integrated POC solution for non-invasive diagnosis and therapy monitoring of Heart Failure patients, KardiaTool) under grant agreement No 768686.

References

1. Cicha I, Lyer S, Janko C, Friedrich RP, Pöttler M, Alexiou C (2017) Magnetic nanoparticles for medical applications. Nanomedicine 12:825–829
2. Rahman MM, Bahadar S, Jamal A, Faisal M, Aisiri M (2011) Iron oxide nanoparticles. In: Rahman M (ed) Nanomaterials. Rijeka, InTech, pp 135–152
3. Bruschi ML, de Toledo LdAS (2019) Pharmaceutical applications of iron-oxide magnetic nanoparticles. Magnetochemistry 5:50
4. Bee A, Massart R, Neveu S (1995) Synthesis of very fine maghemite particles. J Magn Magn Mater 149:6–9
5. Murray CB, Norris DJ, Bawendi MG (1993) Synthesis and characterization of nearly monodisperse CdE (E = sulfur, selenium, tellurium) semiconductor nanocrystallites. J Am Chem Soc 115:8706–8715
6. Park J, Koo B, Hwang Y, Bae C, An K, Park J-G, Park HM, Hyeon T (2004) Novel synthesis of magnetic Fe2P nanorods from thermal decomposition of continuously delivered precursors using a syringe pump. Angew Chem Int Ed 43:2282–2285
7. Deng H, Li X, Peng Q, Wang X, Chen J, Li Y (2005) Monodisperse magnetic single-crystal ferrite microspheres. Angew Chem Int Ed 44:2782–2785
8. Wang S, Zhang B, Su L, Nie W, Han D, Han G, Zhang H, Chong C, Tan J (2019) Subcellular distributions of iron oxide nanoparticles in rat brains affected by different surface modifications. J Biomed Mater Res Part A 107:1988–1998
9. Wu W, Wu Z, Yu T, Jiang C, Kim W-S (2015) Recent progress on magnetic iron oxide nanoparticles: synthesis, surface functional strategies and biomedical applications. Sci Technol Adv Mater 16:1–43
10. Lu AH, Salabas EL, Schüth F (2007) Magnetic nanoparticles: synthesis, protection, functionalization, and application. Angew Chem Int Ed 46:1222–1244
11. Martínez-Banderas AI, Aires A, Teran FJ, Perez JE, Cadenas JF, Alsharif N, Ravasi T, Cortajarena AL, Kosel J (2016) Functionalized magnetic nanowires for chemical and magneto-mechanical induction of cancer cell death. Sci Rep 6:1–11
12. Tarhini M, Greige-Gerges H, Elaissari A (2017) Protein-based nanoparticles: from preparation to encapsulation of active molecules. Int J Pharm 522:172–197
13. Li Z, Qiang L, Zhong S, Wang H, Cui X (2013) Synthesis and characterization of monodisperse magnetic Fe_3O_4 at BSA core–shell nanoparticles. Colloids Surf A Physicochem Eng Aspects 436:1145–1151
14. Gonzalez-Moragas L, Yu S-M, Carenza E, Laromaine A, Roig A (2015) Protective effects of bovine serum albumin on superparamagnetic iron oxide nanoparticles evaluated in the nematode *Caenorhabditis elegans*. ACS Biomater Sci Eng 1:1129–1138
15. Aires A, Ocampo SM, Cabrera D, de la Cueva L, Salas G, Teran FJ, Cortajarena AL (2015) BSA-coated magnetic nanoparticles for improved therapeutic properties. J Mater Chem B 3:6239–6247
16. Nosrati H, Sefidi N, Sharafi A, Danafar H, Kheiri Manjili H (2018) Bovine serum albumin (BSA) coated iron oxide magnetic nanoparticles as biocompatible carriers for curcumin-anticancer drug. Bioorg Chem 76:501–509
17. Montagne F, Mondain-Monval O, Pichot C, Mozzanega H, Elaïssari A (2002) Preparation and characterization of narrow sized (o/w) magnetic emulsion. J Magn Magn Mater 250:302–312
18. Bitar A, Vega-Chacón J, Lgourna Z, Fessi H, Jafelicci M, Elaissari A (2018) Submicron silica shell–magnetic core preparation and characterization. Colloids Surf A Physicochem Eng Aspects 537:318–324
19. Tarhini M, Benlyamani I, Hamdani S, Agusti G, Fessi H, Greige-Gerges H, Bentaher A, Elaissari A (2018) Protein-based nanoparticle preparation via nanoprecipitation method. Materials 11:394–412
20. Barth A, Zscherp C (2002) What vibrations tell about proteins. Q Rev Biophys 35:369–430
21. Qasim M, Asghar K, Dharmapuri G, Das D (2017) Investigation of novel superparamagnetic Ni 0.5 Zn 0.5 Fe_2O_4 @albumen nanoparticles for controlled delivery of anticancer drug. Nanotechnology 28:365101
22. Li D, Hua M, Fang K, Liang R (2017) BSA directed-synthesis of biocompatible Fe 3 O 4 nanoparticles for dual-modal T 1 and T 2 MR imaging in vivo. Anal Methods 9:3099–3104
23. Katumba G, Mwakikunga BW, Mothibinyane TR (2008) FTIR and Raman spectroscopy of carbon nanoparticles in SiO2, ZnO and NiO matrices. Nanoscale Res Lett 3:421–426
24. Wu Z, Xiang H, Kim T, Chun M-S, Lee K (2006) Surface properties of submicrometer silica spheres modified with aminopropyltriethoxysilane and phenyltriethoxysilane. J Colloid Interface Sci 304:119–124
25. Čampelj S, Makovec D, Drofenik M (2009) Functionalization of magnetic nanoparticles with 3-aminopropyl silane. J Magn Magn Mater 321:1346–1350
26. Mikhaylova M, Kim DK, Berry CC, Zagorodni A, Toprak M, Curtis ASG, Muhammed M (2004) BSA immobilization on amine-functionalized superparamagnetic iron oxide nanoparticles. Chem Mater 16:2344–2354
27. Jiang P, Zhang Y, Zhu C, Zhang W, Mao Z, Gao C (2016) Fe_3O_4/BSA particles induce osteogenic differentiation of mesenchymal stem cells under static magnetic field. Acta Biomater 46:141–150
28. Can K, Ozmen M, Ersoz M (2009) Immobilization of albumin on aminosilane modified superparamagnetic magnetite nanoparticles and its characterization. Colloids Surf B Biointerfaces 71:154–159
29. Nosrati H, Salehiabar M, Manjili HK, Danafar H, Davaran S (2018) Preparation of magnetic albumin nanoparticles via a simple and one-pot desolvation and co-precipitation method for medical and pharmaceutical applications. Int J Biol Macromol 108:909–915
30. Souza DM, Andrade AL, Fabris JD, Valério P, Góes AM, Leite MF, Domingues RZ (2008) Synthesis and in vitro evaluation of toxicity of silica-coated magnetite nanoparticles. J Non Cryst Solids 354:4894–4897
31. Bini RA, Marques RFC, Santos FJ, Chaker JA, Jafelicci M (2012) Synthesis and functionalization of magnetite nanoparticles with different amino-functional alkoxysilanes. J Magn Magn Mater 324:534–539

32. Zhu L, Wang D, Wei X, Zhu X, Li J, Tu C, Su Y, Wu J, Zhu B, Yan D (2013) Multifunctional pH-sensitive superparamagnetic iron-oxide nanocomposites for targeted drug delivery and MR imaging. J Control Release 169:228–238
33. Lu HM, Zheng WT, Jiang Q (2007) Saturation magnetization of ferromagnetic and ferrimagnetic nanocrystals at room temperature. J Phys D Appl Phys 40:320–325
34. Yu S, Wu G, Gu X, Wang J, Wang Y, Gao H, Ma J (2013) Magnetic and pH-sensitive nanoparticles for antitumor drug delivery. Colloids Surf B Biointerfaces 103:15–22